Reprinted From Estuarine and Coastal Modeling
Proceedings of the Conference
American Society of Civil Engineers
Held November 3-5, 1999, New Orleans, Louisiana

EFFECT OF HEAT FLUX ON THERMOCLINE FORMATION

Joseph S. Helfand[1], David P. Podber[1], and Michael J. McCormick[2]

ABSTRACT

A numerical model based upon Deardorff (1980) was used to simulate heat transfer between a lake and the atmosphere. The model includes a lake-atmosphere heat exchange submodel, with penetration of solar radiation. Heat and momentum are transferred in the vertical with a one-dimensional model that disregards horizontal processes. Atmospheric forcing to drive the models was taken from NOAA Marobs buoy 45007 in the south central region of Lake Michigan, and from the nearby land based stations at Milwaukee, WI, and Muskegon, MI. Three simulations were run and compared to field data collected by NOAA GLERL in 1996. The simulations focused on the formation of the thermocline from June 9 to August 1. The first simulation used land-based atmospheric data as inputs, the second used buoy data supplemented with land data where needed. The results were compared to the field data and showed that using terrestrial data can lead to results that are plausible, but inaccurate. The third simulation used buoy and land data as before, but adjusted the incoming solar radiation to produce a better fit to the observed data. The adjustment apparently compensated for deficiencies in the land-based data.

INTRODUCTION

Numerical modeling of large lakes, estuaries, coastal waters, and gulfs has advanced to the point that it is now standard to run seasonal simulations with highly resolved spatial (1~10 km) and temporal (30~90 s) scales. The accurate

[1] Limno-Tech, Inc. 501 Avis Drive, Ann Arbor, MI 48108
[2] Great Lakes Environmental Research Laboratory, NOAA, 2205 Commonwealth Blvd., Ann Arbor, MI 48105

computation of the ocean (lake)-atmosphere heat exchange is necessary to compute the development of the thermal structure (i.e., thermocline location) accurately over a seasonal scale. The density stratification associated with thermal stratification affects the circulation patterns produced by the atmospheric input of momentum, which is responsible for the circulation in non-tidal systems and the residual circulation in tidal systems.

A vertical direction, one-dimensional numerical model for velocity, temperature, and turbulence was encoded. The vertical mixing model was the one-equation turbulence model of Deardorff (Deardorff, 1980). The relatively simple 1-equation model of Deardorff was chosen instead of the more sophisticated 2 and 2 ½ equation models (k-ε, or Mellor and Yamada (1974)), to test whether or not a simple mixing scheme is sufficient. Future work is planned to compare the quality of the model results using a suite of models and vertical spacings that are more applicable to a three dimensional model application. A four component heat flux model was used, including incoming solar radiation (short wave), net long wave radiation, evaporative or latent heat, and sensible heat.

Various simulations were run to analyze the sensitivity of the model results to heat flux parameters and data. In particular the effect of land-based versus water-based atmospheric forcings was examined. The model results are compared to the field data, in the form of time series temperatures at various depths, gathered in Lake Michigan by the National Oceanic and Atmospheric Administration (NOAA) Great Lakes Environmental Research Lab (GLERL). The field data used for comparison consisted of velocity and temperature (thermistor) data from a location in the central part of the southern basin of Lake Michigan. This location (Figure 1) was chosen to minimize the advective contribution of heat from the nearshore region, although some advective effects can still be seen in the data.

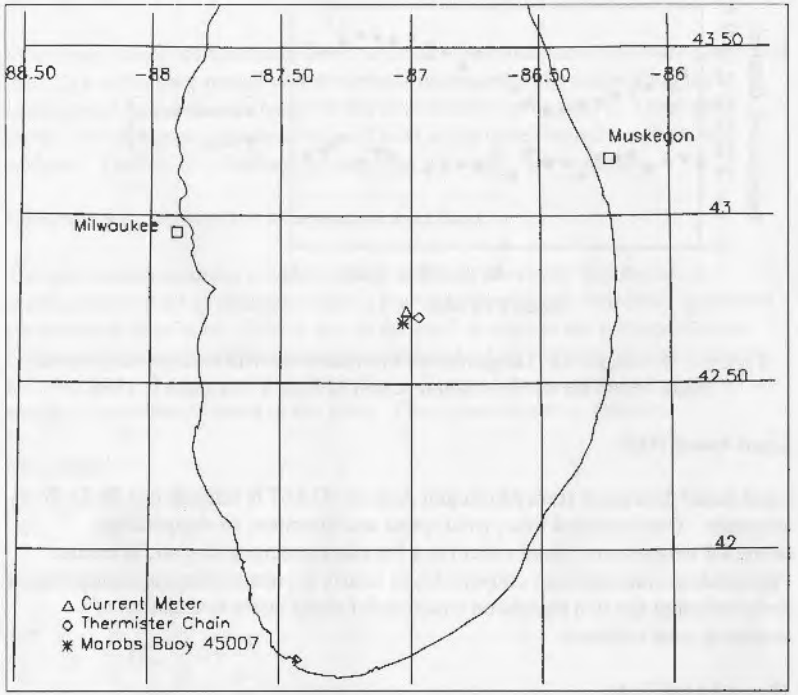

Figure 1: Map of Study Location

DATA

In all cases except for rainfall, linear interpolation of the actual data was used to create hourly data series. For rainfall, hourly precipitation amounts were used as described below. Figure 2 examines air temperatures averaged by the hour over the model period. It is apparent that the land-based data show a clear diurnal cycle, whereas the water-based data show no cycle, in addition to being significantly lower. As will be shown below, data differences between land and water may result in large differences in model results.

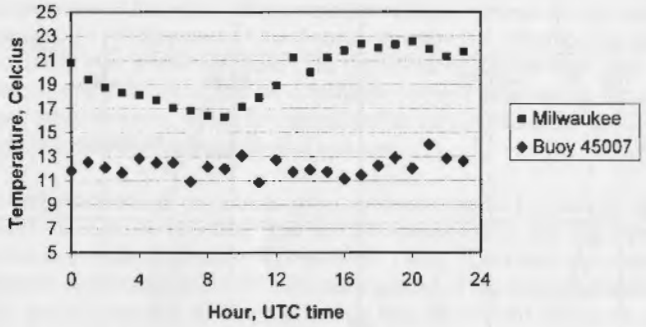

Fignre 2. Averaged Air Temperatures by Hour at the Milwankee Airport and Bnoy 45007 for the simulation period of June 9 – August 1, 1996

Land-based Data

Land-based data came from Muskegon Airport, 43.167 N latitude and 86.25 W longitnde. Data included time, wind speed and direction, air temperatnre, dewpoint temperature, cloud cover (as a fraction), precipitation, and pressure. Precipitation amounts were converted into hourly presence/absence rainfall data for subsequent use in a regression equation for cloud cover attenuation of incoming solar radiation.

Water-based Data

Water-based data came from instruments on a buoy at the study location (42.70 N, 87.00 W), or from surface-moored thermistors at fixed depths nearby (42.697 N, 86.970 W). Atmospheric data included time, wind speed and direction, air temperature, and pressure adjusted to sea level. Pressures were readjusted to an elevation of 198.12 meters (650 feet) using a standard equation (Iribarne and Godson, 1981). Dewpoint temperatures were calculated from the air temperature and an assumed relative humidity of 80 percent, using a curve-fit equation for water vapor pressure as a function of temperature. Thermistor temperatures were collected at depths of 1.3, 3.5, 5.1, 6.7, 8.3, 9.1, 10.0, 11.4, and 13.7 meters at intervals of 15 minutes. Total water depth was about 155 meters. The thermistor data record began June 8, 1996 at hour 2300 EST.

METHODS

Main components of the model are 1) a model for conservation of momentum and heat, 2) a turbulence model which controls mixing, thereby controlling the exchange of heat between water layers at different depths, and 3) a heat flux model, which controls the exchange of heat at the upper boundary (the water surface). The lower boundary is controlled by a zero flux condition.

Governing Equations for Momentum and Heat

The governing equations for momentum and heat are simplified by the assumption that all exchanges occur in the vertical, since all horizontal gradients are assumed to be zero. Effects due to the earth's rotation are neglected since only one direction in the horizontal is addressed. Also vertical advective fluxes are assumed to be zero, so that the vertical fluxes of momentum and heat are due solely to turbulent motions in the fluid. The equations are as follows:

Momentum:

$$\frac{\partial u}{\partial t} = \frac{\partial}{\partial z}(K_m \frac{\partial u}{\partial z})$$

Heat (Temperatnre):

$$\frac{\partial T}{\partial t} = \frac{\partial}{\partial z}(K_h \frac{\partial T}{\partial z}) + \frac{q_s}{\rho c_p}$$

where u(z,t) is the horizontal velocity [m/s], T(z,t) is the temperature [°C], K_m is the vertical eddy viscosity [m^2/s], and K_h is the vertical eddy diffusivity [m^2/s]. K_m and K_h are given by the following relationships, that are explained in the Turbulent Mixing section: $K_m = C_1 \lambda q + K_0$, and $K_h = C_2 K_m$. q, [$W/m^2/m$] is the rate of absorption of the penetrating solar radiation which varies with depth, ρ is the density of water [kg/m^3], and c_p is the heat capacity of water [J/kg/K].

The boundary conditions for the two governing equations are given as:

Surface: $K_m \frac{\partial u}{\partial z}\Big|_s = \frac{\tau_s}{\rho}$, where τ_s is the surface wind stress [Pa],

$K_h \frac{\partial T}{\partial z}\Big|_s = \frac{q_{hf}}{\rho c_p}$, where q_{hf} is the surface heat flux [W/m^2].

Bottom: $u_b = 0.$ $\left.\frac{\partial T}{\partial z}\right|_b = 0.$

Turbulent Mixing in the Vertical

The vertical mixing of momentum and heat was based on the Deardorff (Deardorff, 1980) model, which was also applied more recently by Denbo and Skyllingstad (Denbo and Skyllingstad, 1996). This method can be characterized as a one-equation turbulent kinetic energy (tke) model with an empirically determined mixing length and dissipation rate. The mixing length is based on density stratification, and the dissipation of tke is computed by using the mixing length, empirical constant, and $tke^{-3/2}$.

The governing equation from Deardorff has been modified by dividing through by one-half of the square root of the tke to avoid the computational burden of taking the square root (although this burden is minimal in the one-dimensional application used in this study). The governing equations were also simplified because this study is one-dimensional. The equations are given below:

$$\frac{\partial q}{\partial t} = \underbrace{\frac{K_m}{2q}[P]}_{\text{shear production}} + \underbrace{\frac{\beta g}{2q} K_h \frac{\partial T}{\partial z}}_{\text{buoyant production/ dissipation}} + \underbrace{\frac{\partial}{\partial z}(C_{dq} K_m \frac{\partial q}{\partial z})}_{\text{vertical diffusion of turbulence}} - \underbrace{\frac{\varepsilon}{2q}}_{\text{dissipation rate}}$$

where $q^2 = k = (\overline{u'}^2 + \overline{v'}^2 + \overline{w'}^2)/2.0$, and u', v', w' are the turbulent fluctuations in the u,v,w velocities respectively; $K_m = C_{km}\lambda q + K_0$ is the vertical eddy viscosity [m^2/s], C_{km} is an empirical coefficient, λ is the mixing length, $K_0 = 1.0 \times 10^{-6}$ is the background mixing, $K_h = (C_{hl} + C_{hs}\frac{\lambda}{\Delta s})K_m$ is the vertical eddy diffusivity [m^2/s], C_{hl} and C_{hs} are empirical coefficients, Δs is the vertical grid spacing, P is the prodnction of turbulence due to shear in the mean flow; in tensor notation it is written as $P = (\frac{\partial u_i}{\partial x_j} + \frac{\partial u_j}{\partial x_i})\frac{\partial u_i}{\partial x_j}$, which simplifies to $P = (\frac{\partial u}{\partial z})^2$ for one dimension using standard notation, $\beta = 8.75 \times 10^{-6}$ (T + 9.0) for T in °C., and β has units [1/°C].

The mixing length, λ, is computed differently for stable and unstable conditions, as given below:

Stable Fluid	Unstable Fluid
$\lambda = \begin{cases} l = C_l q\left(\frac{g}{\rho_0}\frac{\partial \rho}{\partial z}\right)^{-1/2} \\ \lambda = \min(l, \Delta s) \end{cases}$	$\lambda = \Delta s$

The dissipation rate ε, is given by

$\varepsilon = \frac{C}{\lambda} q^3$, where the constant $C = \left(C_{el} + C_{es}\left(\lambda / \Delta s\right)\right) C_{wall}$.

The empirical constants were assigned the values described in Deardorff, as follows:

$C_{dq} = 2.0$, $C_{el} = 0.19$, $C_{es} = 0.51$, $C_l = 0.76$, $C_{km} = 0.1$, $C_{hl} = 1.0$, $C_{hs} = 2.0$, C_{wall} = {1.0 away from solid boundaries, 3.9 next to solid boundaries and at the surface.}.

The bonndary conditions imposed on the governing equation are as follows:

Surface conditions for q and P : $\frac{\partial^2 q}{\partial z^2} = 0.$ $P|_s = (\left.\frac{\partial u}{\partial z}\right|_s)^2 = \left[\frac{\tau_s}{\rho K_m}\right]^2$, where τ_s is the wind stress. Bottom conditions are $\frac{\partial q}{\partial z} = 0$ and $P = \varepsilon$ (following ASCE, 1988).

Heat Flux

The heat flux model was derived from a 1988 heat flux model developed by McCormick of the Great Lakes Environmental Research Laboratory as applied to Lake Erie (Kelley, 1995). The model uses standard meteorological observations and snrface water temperatures as model input. Model output consists of two types of components generated by four submodels. The surface flux (equivalent to q_{hf} in the above governing equation bonndary conditions) is the snm of the fluxes from the net long wave radiation, evaporative or latent heat, and sensible heat submodels. The penetrating flux (the source of q_r in the above governing equations) comes from the incoming solar radiation (short wave).

The heat flux model uses a heat balance approach in which the total heat flux is equal to the sum of the shortwave radiation, long wave radiation, sensible heat flux and latent heat flux. The terms, in watts/meter^2, are positive for energy flowing into the lake. In equation form, the model is:

$$H_{total} = H_{SR} + (H_{LR} + H_S + H_L) = \int_{z=0}^{z=h} q_s \, dz + q_N$$

where H_{total} is the net heat flux with the atmosphere, H_{SR} is the net incoming short wave radiation, H_{LR} is the net long wave radiation, H_S is the sensible heat transfer, and H_L is the latent heat transfer.

H_{SR}, Short Wave Radiation

The short wave radiation is a function of clear sky radiation. Clear sky radiation is predicted by a regression equation from the solar zenith angle, and is modified by cloud cover. The resulting equation follows Cotton (1979):

$$H_{SR} = (SR_c)(CLD)$$

where SR_c is the net incoming short wave radiation for clear sky conditions, and CLD is the "cloud effect" term. SR_c is computed from the equation:

$$SR_c = a_0 + a_1\cos(Z) + a_2(\cos(Z))^2 + a_3(\cos(Z))^3$$

where a_0, a_1, a_2, and a_3 are empirical coefficients, and Z is the solar zenith angle (defined as the angular distance of the sun from local vertical). Z is computed following Guttman and Matthews, 1979. CLD is computed from the equation:

$$CLD = c_0 + c_1S_c + c_2(S_c)^2 + c_3(S_c)^3 + c_4(RN)$$

where S_c is the opaque cloud cover amount, c_0, c_1, c_2 , c_3, and c_4 are empirical coefficients, and RN = 0 if it is not raining, RN = 1 if it is.

The attenuation of the short wave radiation in the water column is described by the Beer's law equation:

$$I_{z,\lambda} = I_{0,\lambda} e^{-K_{e,\lambda} z}$$

where $I_{z,\lambda}$ is the light intensity [W/m^2] at depth z, z is the depth [m], $K_{e,\lambda}$ is the extinction coefficient [m^{-1}], $I_{0,\lambda}$ is the incoming solar radiation at the surface, and λ is the wavelength [nm]. The effect on the computed light attenuation of using low resolution or high resolution extinction coefficients was investigated. It was fonnd that the low resolution of just two wavelength bands, infrared and visible/ultraviolet, gave very similar resnlts to using the high resolution of many wavelength bands. Therefore the model was implemented with two wavelength bands, infrared and visible/ultraviolet, with extinction coefficients of 2.85 and 0.296 respectively. The light attenuation is converted to heat as q_s.

H_{LR}, Long Wave Radiation

The net long wave radiation is a function of the water temperature, air temperature and cloud cover. The equation used follows Wyrtki (1965):

$$H_{LR} = -S_{SB}\,\varepsilon\,(T_W^4(0.39\text{-}0.05e_a^{1/2})[1.0\text{-}kS_c^2] + 4T_W^3(T_W\text{-}T_A))$$

where S_{SB} is the Stefan-Boltzmann constant, 5.67051 x 10^{-8} watts/(m^2 K^4), ε is the emissivity assumed equal to 0.97, T_W is the water temperature [K], e_a is the vapor pressnre of air [millibars], k is a parameter that increases linearly with latitude from 0.5 at the equator to 0.8 at 70° of latitude, and T_A is the air temperature [K].

H_S, Sensible Heat

The sensible heat flux is a function of the air-water interface temperature differential, the air density, heat capacity, and the wind speed. The calculation uses a bulk transfer approach according to McBean et al. (1979):

$$H_S = \rho_a C_p C_H U(T_W\text{-}T_A)$$

where ρ_a is the density of air [kg/m^3], Cp is the specific heat of air at constant pressure [J/(kg K)], C_H is the bulk heat transfer coefficient for momentum, U is the wind speed [m/s], T_W is the water temperature, and T_A is the air temperature.

H_L, Latent Heat

The latent heat flux (due to evaporation and condensation) is a function of air density, water latent heat of vaporization, wind speed, water temperature, and air humidity. The equation used (Kelley, 1995) is:

$$H_L = \rho_a L_V C_D U(q_A - q_W)$$

where L_V is the latent heat of vaporization at the temperature of the water surface [J/kg], C_D is the bulk transfer coefficient for momentum, q_A is the specific humidity of the air (ratio of water vapor mass to total humid air mass), and q_W is the specific humidity of the air at the water surface.
The q_A and q_W functions are calculated by:

$$q_A = 0.62185 e_A/(P - 0.37815 e_A)$$
$$q_W = 0.62185 e_W/(P - 0.37815 e_W)$$

where e_A is the saturation vapor pressure [millibars], P is the air pressure, [millibars], and e_W is the saturation vapor pressure of water at T_W, [millibars].

C_D and C_H, Bulk Transfer Coefficients

The dimensionless bulk transfer coefficients for momentum (C_D) and heat (C_H) are used in the calculations of the latent and sensible heat transfer terms, described above. Both C_D and C_H are dependent on the stability of the lowest few meters of the atmospheric boundary layer, the height of wind speed measurement and the wind speed. These coefficients also include the effects of surface roughness. C_D is determined from the equation:

$$C_D = \frac{u^{*2}}{u_z^2}$$

where u* is the friction velocity [m/s], and u_z is the wind speed at height z. C_H is calculated as a function of the dimensionless stability height using parameters developed in the calculation of C_D. A profile method is used to estimate u* (Schwab, 1978; Lui and Schwab, 1987). The method is based on Monin-Obukhov similarity theory (Monin and Obukhov, 1954) and on the works of Businger et al. (1971), Long and Shaffer (1975), Panofsky (1963), Paulson (1970), and Smith and Banke (1975).

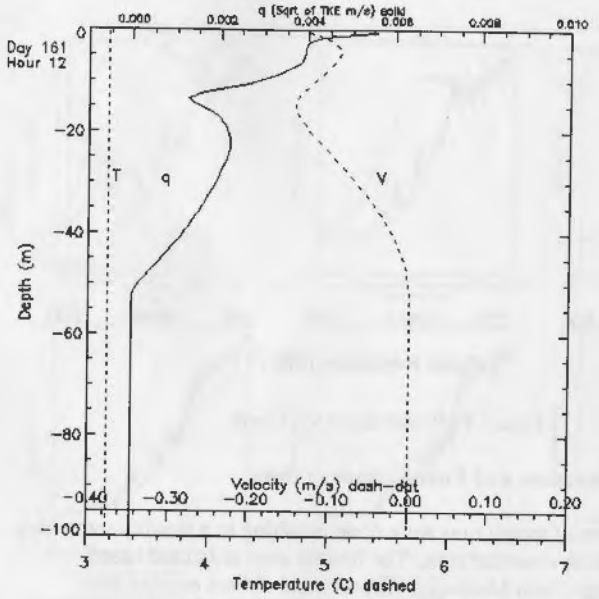

Figure 3: Turbulence Variables vs. Depth

RESULTS

Overview of Runs

Model runs were done for the period Julian day 161 (June 9, 1996), hour 0400 UTC, to day 214 (August 1, 1996), hour 0000 UTC. Figure 3 shows an example of turbulence-related variables (temperature, velocity, and q) versus depth. Figure 4 shows an example of average penetrating solar radiation power input estimated by the heat flux model versus depth.

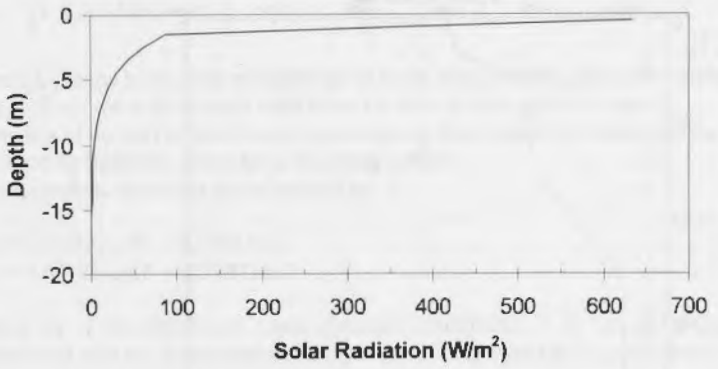

Figure 4: Power Input vs. Depth

Data Choice, Calibration, and Comparisons to Data

A series of three sets of model runs were done, resulting in a steadily improving fit of model outputs to observed data. The first set used only land-based atmospheric forcings (from Muskegon Airport), and did not employ any calibration of model to data (other than original literature empirical constants). The second set used the available atmospheric forcings recorded at the buoy, along with the land-based cloud cover and rainfall (which were not recorded at the buoy). The third set used the same forcings as the second, except that solar input was reduced by 50 percent for the first 17 days in accordance with the observation that the observed water temperature data indicated a markedly lower heat input during this period. During the first 17 days there are small diurnal variations in the surface water temperature that can be explained by a radiative heat flux of 30-40 W/m^2. It is surmised that the small amount of radiative heat flux was due to a thicker cloud cover over the lake than was reported at the Muskegon airport. Fog over the lake is a common spring time feature, and was accounted for by increasing the cloud cover where needed.

The first two sets are compared to data in Figure 5, which shows temperature vs. time at thermistor depths. The land-based forcing produces results which are plausible but inaccurate. The buoy+land forcing produces more accurate results. It is apparent, especially at greater depths, that some features of the data (e.g. high-frequency variability due to internal waves) are due to horizontal processes which the present vertical application cannot resolve.

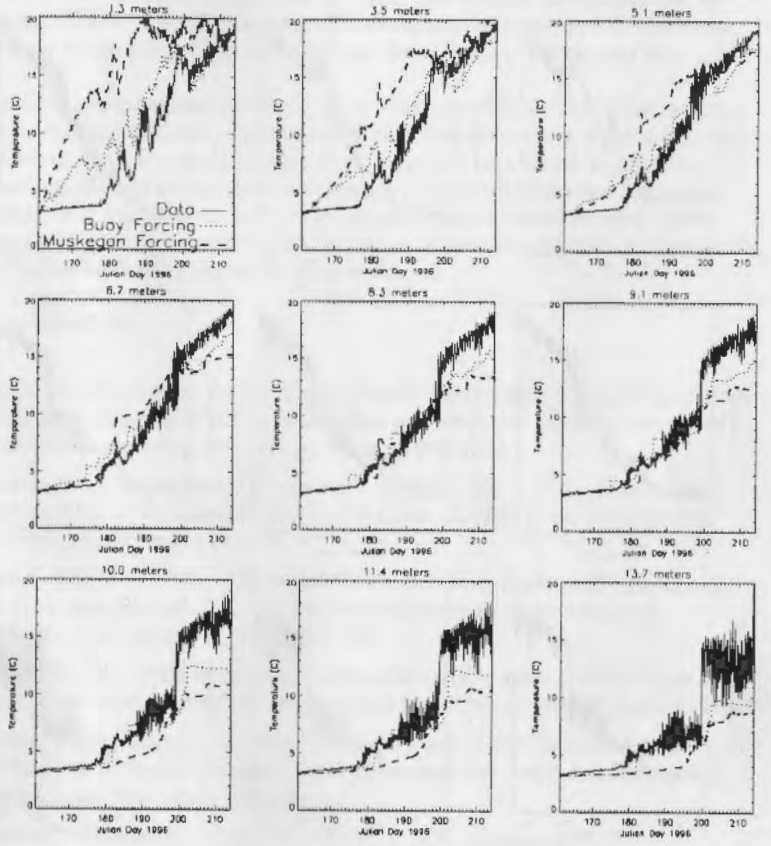

Figure 5: Model vs. Data with Forcings from Two Locations

The third set is compared to data in Figure 6. The adjustment made in this third set apparently compensates for deficiencies in the land-based cloud cover data during this period, resulting in a much-improved fit of model to data.

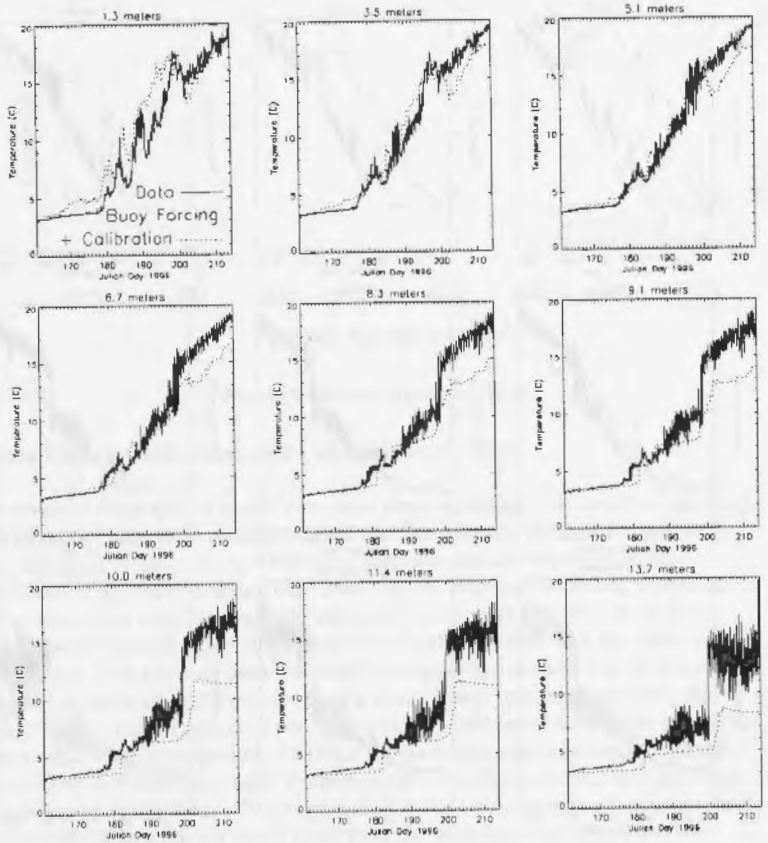

Figure 6: Model vs. Data with Calibration of Solar Input

CONCLUSIONS

Currently available numerical models are able to simulate thermocline formation accurately, given accurate forcing functions. The predictive capabilities of the models are limited by the accuracy of the available data. The use of terrestrial data will lead to thermal structures that may be plausible but inaccurate.

The top few meters of the lake tend to equilibrate with the atmosphere and are insensitive to horizontal processes. This is not true for lower layers, which are strongly influenced by internal waves and the collapse of the thermal bar.

The level one turbulence closure scheme of Deardorff tended to inhibit mixing across the thermocline to a greater extent than data indicates it ought to be. Some sensitivity analysis was performed on the empirical coefficients reported by Deardorff, though not reported in this article. The results from those analyses indicate that it is possible to adjust those coefficients to better simulate site-specific physics. It should be noted that, even with no modification to Deardorff's empirical coefficients, the model performed well.

REFERENCES

ASCE Task Committee on Turbulence Models in Hydraulic Computations: 1988. *Turbulence modeling of surface water flow and transport: parts i-v.* Journal of Hydraulic Engineering, vol. 114, no. 9, pages 970-1073.

Businger, J.A.; Wyngaard, J.C.; Izumi, Y.; Bradley, E.F.: 1971. *Flux-Profile Relationships in the Atmospheric Surface Layer.* Journal of the Atmospheric Sciences, vol. 28, pages 181-189.

Cotton, Gerald F.: 1979. *ARL Models of Global Solar Radiation, Appendix VI.* Air Resources Laboratories, Environmental Research Laboratories, U.S. Department of Commerce, pages 165-184.

Deardorff, J.W.: 1980. *Stratocumulus-Capped Mixed Layers Derived From a Three-Dimensional Model.* Boundary-Layer Meteorology, vol. 18, pages 495-527.

Denbo, D.; Skyllingstad, E.: 1996. *An Ocean Large-Eddy Simulation Model with Applications to Deep Convection in the Greenland Sea.* Journal of Geophysical Research, vol. 101, pages 1095-1110.

Guttman, Nathaniel B.; Matthews, J. David.: 1979. *Computation of Extraterrestrial Solar Radiation, Solar Elevation Angle, and True Solar Time of Sunrise and Sunset, Appendix II.* National Climatic Center, Environmental Data and Information Service, U.S. Department of Commerce, pages 47-54.

Iribarne, J.V., Godson, W.L.: 1981. *Atmospheric Thermodynamics.* 2nd Edition. 259 pages.

Kelley, John Gormley Walsh: 1995. *One-Way Coupled Atmospheric-Lake Model Forecasts For Lake Erie.* Dissertation. Ohio State U., 450 pages.

Liu, Paul C.; Schwab, David J.: 1987. *A Comparison of Methods for Estimating u_* From Given u_z and Air-Sea Temperature Differences.* Journal of Geophysical Research, vol. 92, no. C6, pages 6488-6494.

Long, Paul E. Jr.; Shaffer, Wilson A.: 1975. *Some Physical and Numerical Aspects of Boundary Layer Modeling.* NOAA Tech. Memo. NWS TDL-56, 37 pages.

McBean, G.A.; Bernhardt, K.; Bodin, S.; Litynska, Z.; Van Ulden, A.P.; Wyngaard, J.C.: 1979. *The Planetary Boundary Layer (Technical Note No. 165).* World Meteorological Organization, no. 530, 200 pages.

Mellor, G.; Yamada, T.: 1974. *A Hierarchy of Turbulence Closure Models for Planetary Boundary Layers.* Journal of the Atmospheric Sciences, vol. 31, pages 1791-1806.

Monin, A.S.; Obukhov, A.M.: 1954. *Basic Laws of Turbulent Mixing in the Atmosphere Near the Ground.* Tr. Akad. SSSR Geofiz. Inst. vol. 24, pages 163-187.

Paulson, C.A.: 1970. *The Mathematical Representation of Wind Speed and Temperature Profiles in the Unstable Atmospheric Surface Layer.* J. Appl. Meteor., vol. 9, pages 857-861.

Panofsky, H.A.: 1963. *Determination of Stress From Wind and Temperature Measurements.* Quat. J. Meteorol. Soc., vol. 89, pages 85-94.

Schwab, David J.: 1978. *Simulation and Forecasting of Lake Erie Storm Surges.* Monthly Weather Review, vol. 106, no. 10, pages 1476-1487.

Smith, S.D., Banke, E.G.: 1975. *Variation of the Sea Surface Drag Coefficient With Wind Speed.* J. R. Met. Soc., vol. 101, pages 665-673.

Wyrtki, Klaus: 1965. *The Average Annual Heat Balance of the North Pacific Ocean and Its Relation to Ocean Circulation.* Journal of Geophysical Research, vol. 70, no. 18, pages 4547-4559.

ACKNOWLEDGMENT

The authors would like to acknowledge the Donald C. Cook Nuclear Plant, Bridgman, Michigan for its support for the development of the heat flux algorithms.